

Article

Comparative In Vitro Analysis of Composite Resins Used in Clear Aligner Attachments

Francesca Gazzani ¹, Denise Bellisario ^{2,*} , Chiara Pavoni ¹ , Loredana Santo ² , Paola Cozza ¹ and Roberta Lione ¹ 

¹ Department of Faculty of Medicine and Surgery, UniCamillus International Medical University, 00131 Rome, Italy; francesca.gazzani@unicamillus.org (F.G.); chiara.pavoni@unicamillus.org (C.P.); paola.cozza@unicamillus.org (P.C.); roberta.lione@unicamillus.org (R.L.)

² Department of Industrial Engineering, University of Rome "Tor Vergata", 00133 Rome, Italy; loredana.santo@uniroma2.it

* Correspondence: denise.bellisario@uniroma2.it or denise.bellisario@unimercatorum.it

Abstract

Background: Attachments are essential components in clear aligner therapy, enhancing retention and improving the predictability of tooth movements. Mechanical and wear properties of the composite resins used for attachment reproduction are critical to maintaining their integrity and shape over time. This study aimed to evaluate and compare the mechanical properties, thermal behavior, and wear performance of the hybrid composite Aligner Connect (AC) and the flowable resin (Connect Flow, CF). **Methods:** Twenty samples (ten AC and ten CF) were reproduced. All specimens underwent differential scanning calorimetry (DSC), combustion analysis, flat instrumented indentation, compression stress relaxation tests, and tribological analysis. A 3D wear profile reconstruction was performed to assess wear surfaces. **Results:** DSC and combustion analyses revealed distinct thermal transitions, with CF showing significantly lower Tg values (103.8 °C/81.4 °C) than AC (110.8 °C/89.6 °C) and lower residual mass after combustion (23% vs. 61%), reflecting reduced filler content and greater polymer mobility. AC exhibited superior mechanical properties, with higher maximum load (585.9 ± 22.36 N) and elastic modulus (231.5 ± 9.1 MPa) than CF (290.2 ± 5.52 N; 156 ± 10.5 MPa). Stress relaxation decrease was less pronounced in AC (18 ± 4%) than in CF (20 ± 4%). AC also showed a significantly higher friction coefficient (0.62 ± 0.060) than CF (0.55 ± 0.095), along with greater wear volume (0.012 ± 0.0055 mm³ vs. 0.0070 ± 0.0083 mm³) and maximum depth (36.88 ± 3.642 μm vs. 17.91 ± 3.387 μm). Surface roughness before wear was higher for AC (Ra, 0.577 ± 0.035 μm; Rt, 4.369 ± 0.521 μm) than for CF (Ra, 0.337 ± 0.070 μm; Rt, 2.862 ± 0.549 μm). After wear tests, roughness values converged (Ra, 0.247 ± 0.036 μm for AC; Ra, 0.236 ± 0.019 μm for CF) indicating smoothed and similar surfaces for both composites. **Conclusions:** The hybrid nanocomposite demonstrated greater properties in terms of stiffness, load-bearing capacity, and structural integrity when compared with flowable resin. Its use may ensure more durable attachment integrity and improved aligner–tooth interface performance over time.

Keywords: nanocomposite resins; clear aligner treatment; attachments; tribological analysis; wear of polymers



Academic Editor: Maria Pia Ferraz

Received: 1 July 2025

Revised: 1 August 2025

Accepted: 4 August 2025

Published: 6 August 2025

Citation: Gazzani, F.; Bellisario, D.; Pavoni, C.; Santo, L.; Cozza, P.; Lione, R. Comparative In Vitro Analysis of Composite Resins Used in Clear Aligner Attachments. *Appl. Sci.* **2025**, *15*, 8698. <https://doi.org/10.3390/app15158698>

Copyright: © 2025 by the authors. Licensee MDPI, Basel, Switzerland. This article is an open access article distributed under the terms and conditions of the Creative Commons Attribution (CC BY) license (<https://creativecommons.org/licenses/by/4.0/>).

1. Introduction

Nowadays, nanocomposite materials are increasingly used in orthodontic treatments for their favorable mechanical performance, aesthetics, and adaptability to various clinical demands [1,2]. In clear aligner treatment (CAT), they play a crucial role in the reproduction of attachments, which are essential for transmitting orthodontic forces to the teeth and controlling complex movements [1–4]. The interaction between the aligner surface and attachments enhances aligner fit and consequently improves the control of planned orthodontic forces [5]. Since all aligners are designed and manufactured based on the attachment positions of the initial template, any inaccuracies during the first bonding phase can lead to improper tooth movements, which subsequent aligners are unable to compensate for throughout the treatment [6]. In a recent investigation, Weckmann et al. [6] concluded that the bonding protocol may influence the precision of attachments, suggesting the use of low-viscosity composites or a two-phase procedure to achieve more accurate results. Furthermore, the shape, configuration, and positioning of attachments should be carefully preserved during treatment to ensure their intended function is fulfilled. In clinical practice, several factors may lead to a premature attachment failure, including detachment, shape deformation, and reduced aligner adaptation. Accordingly, their performance is also influenced by physico-chemical and mechanical characteristics of the nanocomposite materials which they are made from [1,7–9]. The selection of a material with optimal properties is undoubtedly crucial for securing both durability and functional performance of the mentioned auxiliary elements during treatment [10]. Resin composites consist mainly of the following three components: an organic resin matrix, inorganic filler particles, and a coupling agent. Flowable composites share the same chemical structure but contain a lower amount of filler compared to conventional ones. Numerous studies [4,5,10,11] have evaluated the effectiveness of various resin-based composites used for this purpose. According to D'Antò et al. [4], the viscosity of composite materials does not affect the shape or volume of the attachments. By contrast, more recent findings by Gazzani et al. [2], who compared two nanocomposite resins differing in viscosity and filler content, revealed that conventional composites with higher viscosity exhibit superior wear resistance, making them more suitable for clinical use. Recent advances in dental material science have led to the introduction of more innovative resin-based nanocomposites specifically formulated for use with clear aligner systems [11,12]. Despite the wide adoption of attachments in CAT, few studies have systematically analyzed how differences in composite composition—particularly between flowable and hybrid nanocomposites—impact the mechanical integrity and long-term retention of attachments [2,4,11,12]. Conventional and flowable nanocomposites currently represent the most frequently used resins for attachment reproduction [1,2,13–15], despite their differences in filler volume and viscosity. The composition of flowable resins allows for easier distribution of the composite within the attachment template. However, they exhibit lower wear resistance and stability when compared with conventional materials [2,3]. Gazzani et al. [2] highlighted the significantly superior performance and mechanical resistance of conventional nanocomposites over flowable resins following mechanical testing. More recently a new composite, Aligner Connect (AC), has been introduced, featuring intermediate characteristics between flowable and conventional resins with the aim of combining ease of handling with improved mechanical performance. AC exhibits mechanical properties comparable to those of conventional resins, while presenting an intermediate viscosity level. To date, no comparative studies have explored the mechanical, thermal, and tribological behavior of AC in relation to Connect Flow (CF), a commonly used flowable resin for attachments. Understanding these differences is clinically relevant as superior mechanical strength and wear resistance

can enhance aligner retention and minimize attachment deformation, ultimately improving the predictability of tooth movements.

Therefore, this study addresses this gap by evaluating and comparing the mechanical properties, thermal behavior, and wear performance of AC and CF. We hypothesize that the hybrid composite AC, due to its higher filler content and intermediate viscosity, will demonstrate superior stiffness, load-bearing capacity, and wear resistance compared to the flowable CF, ultimately leading to improved long-term stability and predictability of orthodontic attachments in CAT. The evaluation of mechanical characteristics and their correlation with material compositions provides significant insights that can guide the selection of optimal composite materials, improving the clinical performance of clear aligners. Hence, the primary objective of this study is to investigate the mechanical and tribological performance of two advanced nanohybrid dental composites—Aligner Connect (AC) and Connect Flow (CF)—specifically developed for use in orthodontic attachment applications. Despite the growing adoption of aligner-based treatments, the performance of attachment materials under the functional and mechanical conditions specific to this application remains largely underexplored. For this reason, the present work introduces a dedicated testing methodology, designed and validated by authors in previous studies, to evaluate the multi-scale mechanical integrity and wear resistance of composite materials under conditions simulating the functional demands of orthodontic attachments [1,2]. Key aspects of the novelty include the layer-by-layer fabrication of standardized specimens using custom 3D-printed photomasks, simulating clinically relevant curing depths and conditions; a combined approach integrating flat indentation, stress relaxation, and reciprocating wear tests to capture both quasi-static and time-dependent mechanical responses; and a quantitative wear assessment using 3D surface profilometry and advanced image reconstruction tools. By focusing on materials specifically engineered for direct bonding on enamel and functional retention within aligners, this study provides new insights into the structure–property–function relationships of modern orthodontic composites. The outcomes are expected to guide both clinical material selection and future composite design for improved durability, comfort, and treatment efficiency.

2. Materials and Methods

The experimental analysis was carefully defined to highlight the specific characteristics of the two composites that most significantly impact their performance during orthodontic treatment. The material performance was evaluated based on mechanical and thermal properties assessed during testing. Additionally, a comparative analysis was carried out to underscore the differences in behavior between the two materials.

2.1. Sample Preparation

A total of twenty nanocomposite specimens were fabricated for the experimental investigation, divided equally between two commercially available formulations: Aligner Connect (AC) and Connect Flow (CF). In particular, five samples of each type were prepared for the tribological and mechanical tests and five samples were fabricated for the thermal analysis. To meet the photopolymerization requirements specific to each composite, the deposition process was performed in sequential layers, with a maximum thickness of approximately 1 mm per layer, to ensure full-depth curing and minimize internal stresses.

Custom-designed photomasks with stepped cavities were employed to standardize sample geometry and optimize the curing process. These masks were fabricated using Fused Deposition Modeling (FDM) with a Prusa 3K 3D printer (Prusa Research a.s., Parvizánská 188/7a, Holešovice, Czech Republic) and gray PLA (Polylactic Acid) filament. Each mask featured five cylindrical cavities of 6 mm diameter, a size selected to provide suf-

efficient contact area for macroscopic mechanical testing, such as indentation and tribological assessments (Figure 1a).

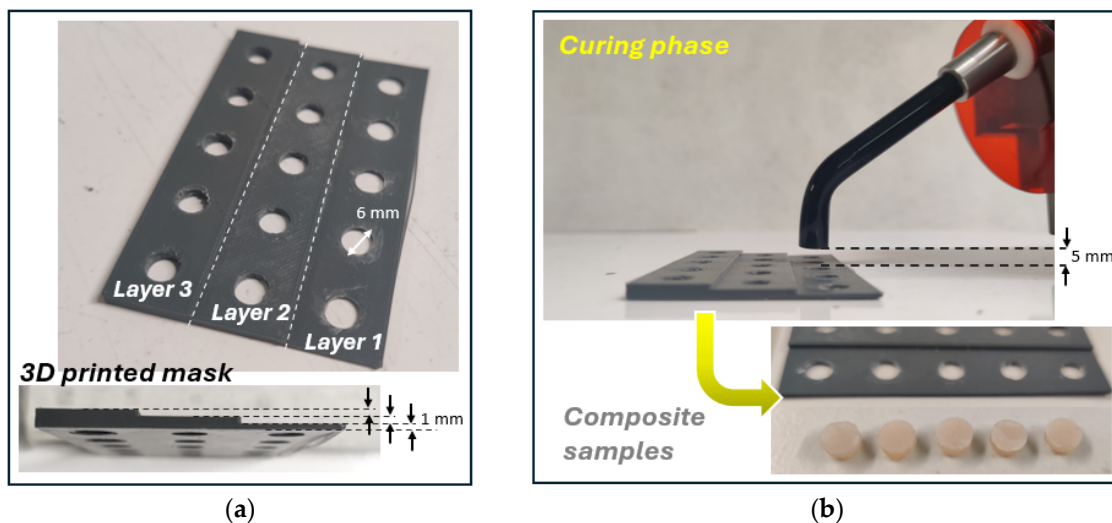


Figure 1. Samples fabrication: (a) 3D printed mask for the three-layer curing phase; (b) curing phase and sample extraction.

The composite material was incrementally dispensed into the mask cavities in three distinct 1 mm-thick layers. Each layer was individually polymerized using a TPC LED (Light-Emitting Diode) curing unit (TPC Advanced Technology, Inc., 851 S. Lawson St City of Industry, CA, USA) delivering an irradiance of 800 mW/cm^2 , positioned at a distance of 5 mm above the surface. A 25 s exposure time per layer was applied to ensure complete polymerization and proper interlayer bonding (Figure 1b). After curing, the samples were demolded and subjected to dimensional and mass measurements using a digital caliper ($\pm 0.01 \text{ mm}$) and a precision balance ($\pm 0.1 \text{ mg}$). These measurements were used to calculate average sample dimensions, volume, and density, enabling consistent comparison across material groups. No additional superficial treatment was performed as the self-leveling properties of the material enabled testing without further preparation. Furthermore, all tests were conducted within 2 h of fabrication, during which time the samples were stored in a closed environment at $25 \text{ }^\circ\text{C}$ and 40% relative humidity.

2.2. Thermal Analysis and Filler Content Determination

To investigate the thermal behavior of the cured nanocomposites, Differential Scanning Calorimetry (DSC) was performed using a DSC 7 system (PerkinElmer, 850 E Collins Blvd, Richardson, TX, USA). Following the curing process, approximately 20 mg of each composite formulation was subjected to double thermal scanning under a nitrogen atmosphere, with a temperature range of $20\text{--}250 \text{ }^\circ\text{C}$ and a heating and cooling rate of $10 \text{ }^\circ\text{C/min}$. The analysis focused on identifying thermal transitions, such as glass transition temperature (T_g) and overall thermal stability of the two composites, also above the range of in vivo use. This was necessary to have a comparison from the point of view of the matrix nature and the effect of the fillers on thermal behavior.

In addition, to quantify the inorganic filler content combustion analysis was carried out. Samples weighing 150 mg were placed in a muffle furnace and heated at $600 \text{ }^\circ\text{C}$ for 60 min to burn off the polymer matrix. The remaining residual mass—representing the inorganic content—was recorded post-cooling to determine the filler weight fraction. This method provided an indirect measure of the reinforcement phase within each composite formulation.

2.3. Mechanical Testing

2.3.1. Indentation Testing

To evaluate the surface mechanical response of the cured composites, flat instrumented indentation tests were conducted using a universal testing machine (Insight/5, MTS Systems S.r.l., Strada Pianezza, 289, Torino, Italy) equipped with a 1 mm diameter flat tungsten carbide indenter and a load cell of 2.5 kN. Tests were performed on the flat top surface of five specimens per material type, which were fixed on a ceramic support.

Each indentation followed a controlled displacement mode, with a preload of 1 N, a loading rate of 0.1 mm/min, and a maximum penetration depth of 0.3 mm (10% of total sample thickness) to limit substrate influence. Upon reaching the target depth, the indenter was retracted to its initial position. The recorded force–displacement data were used to extract parameters such as hardness and stiffness (Figure 2).

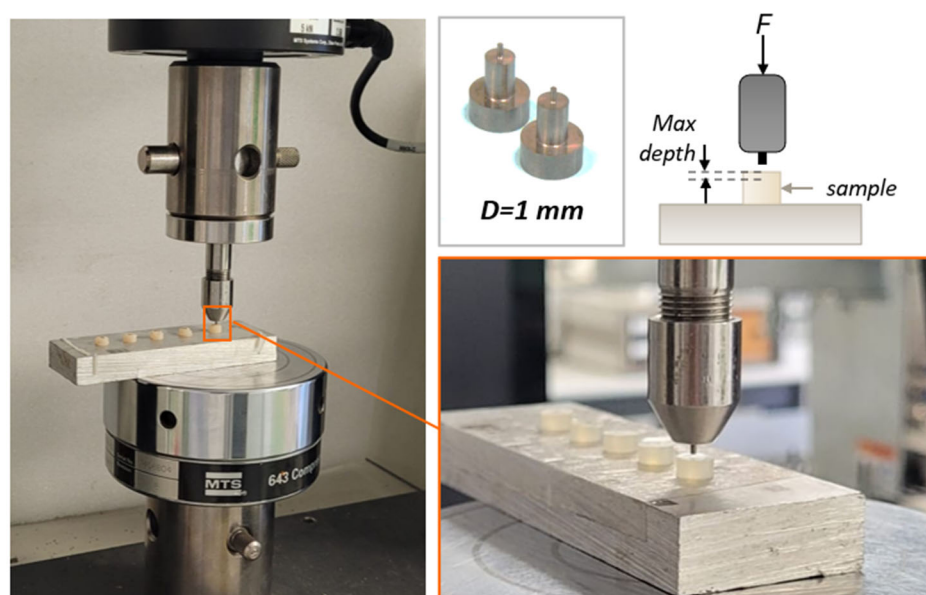


Figure 2. Flat indentation test: schematic representation and picture of the mechanical test on fabricated samples.

2.3.2. Compression Stress Relaxation

To assess the viscoelastic behavior of the composites under compressive loading, stress relaxation tests were performed using a universal testing machine (Alliance/50, MTS Systems S.r.l., Strada Pianezza, 289, Torino, Italy) in compression mode. Five samples per composite type were compressed between parallel plates until a maximum compressive stress of 50 MPa was achieved, with a load cell of 10 kN and a loading rate of 0.1 mm/min. The samples were tested in the absence of a substrate in order to evaluate only the macroscopic viscoelastic behavior of the composites. The machine then held a fixed crosshead position, and the decay in stress over a 15 min time span was continuously recorded. This test enabled the evaluation of time-dependent mechanical properties, indicative of structural relaxation behavior.

2.4. Tribological Testing and Wear Assessment

The wear resistance of the nanocomposites was investigated using dry sliding tribological tests conducted on five samples from each formulation. Tests were carried out with a Linear Reciprocating Tribometer (CSM Instruments, Rue de la Gare 4, Peseux, Switzerland) under ambient conditions (20 °C temperature and 40% relative humidity). Each specimen was subjected to a normal load of 10 N using a 6 mm diameter alumina ball as the

counter-face. A reciprocating motion was applied with a stroke length of 4 mm and a frequency of 2.5 Hz for a total of 10,000 cycles. Following testing, the worn tracks were characterized using a contact surface profilometer (TalySurf CLI 2000, Taylor Hobson, UK) to reconstruct detailed 3D wear profiles at a lateral resolution of 5 μm . Wear parameters including maximum and mean wear depth, worn area, and volume loss were quantified using Software TalyMap[®] 9 (Software Update (V9.2.9994)), providing a comprehensive assessment of material removal mechanisms and comparative wear resistance across the two formulations. Additionally, surface roughness was evaluated both before and after the wear test using the same instrument (TalySurf CLI 2000, Taylor Hobson Ltd., 2 New Star Road, Leicester, UK) and identical 3D acquisition resolution. The analysis employed the software TalyMap and a Gaussian filter with a cutoff of 0.08 μm .

3. Results

3.1. Thermal Analysis and Combustion Testing

Figure 3 presents the DSC (differential scanning calorimetry) thermograms for the Aligner Connect (AC) and Connect Flow (CF) composites, detailing their heat flow profiles over the 20–250 $^{\circ}\text{C}$ temperature range at a constant heating rate of 10 $^{\circ}\text{C}/\text{min}$. These curves offer key insights into the materials' thermal transitions, phase behavior, and chemical composition.

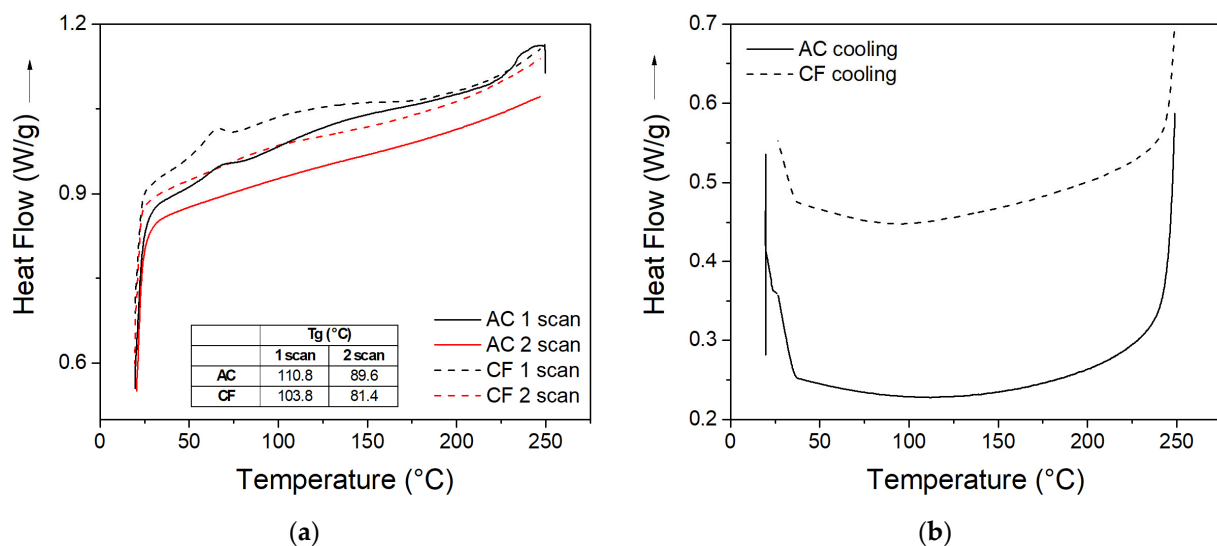


Figure 3. DSC curves 1 scan and 2 scan for AC and CF samples, with endo up (a); cooling curves for AC and CF samples (b).

The thermal behavior of the AC and CF composites was evaluated through DSC analysis, as shown in Figure 3a,b. Both materials exhibited an initial increase in heat flow around 30–70 $^{\circ}\text{C}$ during the first heating scan, which was absent in the second scan. This feature is indicative of residual thermal activity, likely related to moisture release, minor reorganization of the polymer network, or low-temperature relaxation phenomena. A more prominent endothermic event was observed in both composites within the 85–120 $^{\circ}\text{C}$ range, corresponding to the glass transition temperature (T_g) of the polymer matrix. The T_g of CF was slightly lower than that of AC, as reported in the inset table of Figure 3a, with values of 103.8 $^{\circ}\text{C}$ (first scan) and 81.4 $^{\circ}\text{C}$ (second scan) for CF compared to 110.8 $^{\circ}\text{C}$ and 89.6 $^{\circ}\text{C}$ for AC. The CF thermogram displayed a sharper and more pronounced T_g, suggesting a polymer matrix with reduced crosslink density and greater segmental mobility related to the lower presence of filler. Conversely, the broader and more gradual T_g transition in AC may reflect a more heterogeneous network, potentially due to higher crosslink density or

filler–matrix interphase interactions that restrict chain motion. Additionally, CF consistently exhibited higher baseline heat flow than AC, which could be attributed to its lower filler content and greater polymer chain mobility. This trend is further confirmed by the second scan (Figure 3a), where the two materials display different post-T_g thermal responses. At temperatures exceeding ~180 °C a secondary increase in heat flow was noted, particularly for CF. This behavior may point to late-stage, post-curing, residual oligomer reactivity or the onset of thermal softening, consistent with a less thermally stable and more reactive network. In contrast, AC maintained a more subdued heat flow rise, indicating a more thermally inert system. The cooling scans (Figure 3b) further highlight the distinct thermal behaviors. CF retained higher heat flow throughout the cooling phase, consistent with its higher thermal responsiveness and more flexible structure. The flatter cooling curve of AC suggests a more rigid and thermally dampened matrix, likely influenced by its elevated inorganic filler content.

To support these interpretations, combustion analysis was conducted by incinerating 150 mg of cured composite at 600 °C for 60 min. The AC composite retained 61% of its initial mass, whereas CF retained only 23%, confirming a significantly higher inorganic content in AC. This aligns with the DSC findings, where AC's reduced heat flow and broader transitions correlate with its higher filler loading. These fillers are likely inert at test temperatures and act as thermal dampeners, reducing matrix flexibility and suppressing thermal events. In contrast, the lower filler content in CF allows for more pronounced thermal activity, increased heat absorption, and sharper transitions, making it potentially better suited for applications requiring thermal responsiveness or elasticity.

3.2. Mechanical Testing Results

The cylindrical samples were measured to determine the average size and the composite density (Table 1). In terms of material density, AC exhibited a value of 1.50 ± 0.02 g/cm³, while CF showed a lower density of 1.30 ± 0.03 g/cm³. This difference likely contributes to the variations in mechanical and physical properties observed between the two materials.

Table 1. Average dimensions and densities measured for the fabricated composite samples.

Sample	Height (mm)	Diameter (mm)	Density (g/cm ³)
AC	2.7 ± 0.08	6.5 ± 0.15	1.50 ± 0.02
CF	3.0 ± 0.04	6.2 ± 0.05	1.30 ± 0.03

3.2.1. Flat Indentation

Flat indentation tests were used to evaluate the resistance of the composites to localized compressive stress. Figure 4a illustrates the load–displacement curves, and the key performance metrics are reported in Table 2. All the samples underlined a similar behavior for each composite type. At a constant penetration depth of 0.3 mm, the maximum load sustained by AC (585.9 ± 22.36 N) was approximately double that of CF (290.2 ± 5.52 N). This significant difference reflects the greater stiffness of AC, likely due to its higher filler loading and stronger polymer network.

The elastic modulus, derived from the slope of the linear region of the curve, also favored AC (231.5 ± 9.1 MPa) over CF (156 ± 10.5 MPa), confirming its superior resistance to deformation. Meanwhile, the residual indentation depth was slightly lower in AC (0.09 mm) than in CF (0.11 mm), suggesting better elastic recovery. Flat indentation testing revealed that AC exhibited approximately double the maximum load capacity and a substantially higher elastic modulus than CF. These properties make AC particularly suitable for applications demanding rigid mechanical anchorage, such as load-bearing orthodontic attachments or occlusal contact zones. CF, while softer and less stiff, displayed

a slightly greater residual deformation and stress relaxation. Its stress reduction rate (20%) was marginally higher than that observed for AC (18%), suggesting a more pronounced viscoelastic behavior—again consistent with a more flexible and less crosslinked network. These characteristics may be advantageous for attachments subjected to repetitive stress, bending, or interfacial movement, where material adaptability can reduce the risk of fracture or detachment.

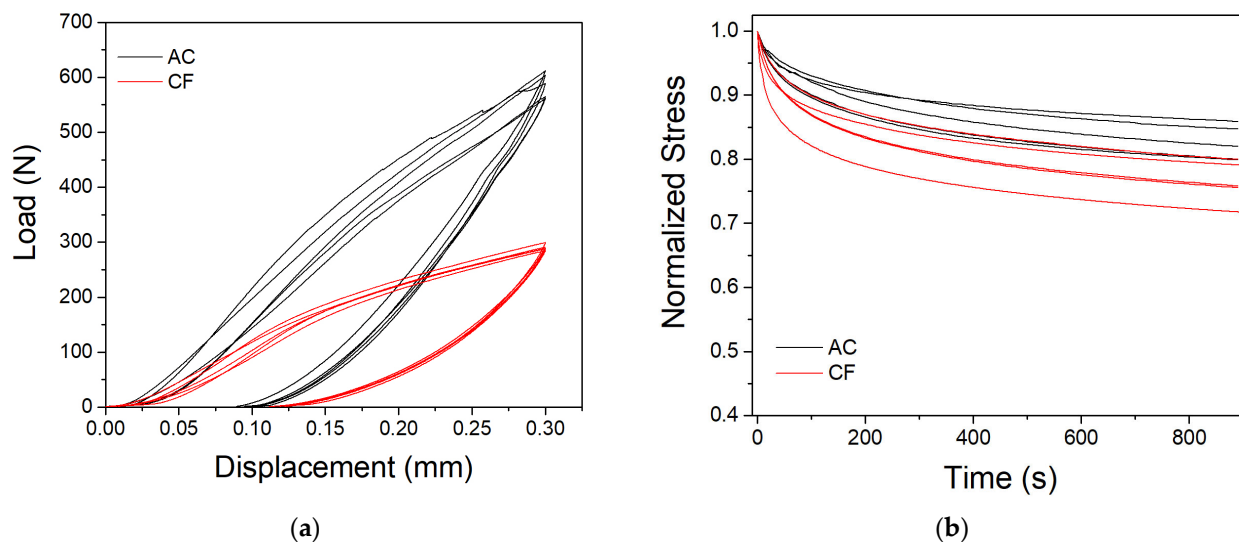


Figure 4. Mechanical test results: (a) loading and unloading curves of flat indentation tests; (b) stress relaxation curves for AC and CF samples.

Table 2. Average dimensions and densities measured for the composite samples.

Sample	Max Load (N)	Elastic Modulus (MPa)	Residual Displacement (mm)
AC	585.9 ± 22.36	231.5 ± 9.1	0.09 ± 0.012
CF	290.2 ± 5.52	156 ± 10.5	0.11 ± 0.007

3.2.2. Stress Relaxation

Figure 3b presents the normalized stress relaxation curves for CF and AC. All stress values were normalized with respect to the initial stress (σ_0), allowing each curve to begin at a dimensionless value of 1. This normalization facilitated a direct comparison across samples. From the curve analysis, AC samples demonstrated a more stable and consistent stress relaxation behavior compared to CF. As with the indentation tests, the high repeatability of the curves for both materials reinforces the reliability of the results and suggests that the differences in mechanical response are intrinsic to the material compositions rather than due to experimental variability. CF featured $20 \pm 4\%$ of stress reduction, while AC showed a lower reduction equal to $18 \pm 4\%$.

The observed mechanical differences reflect variations in network design and filler architecture, rather than being solely attributed to material stiffness. The greater repeatability of the mechanical response across all specimens suggests intrinsic material differences, rather than fabrication variability. Moreover, the consistency of the results across multiple tests indicates that the behavior is not attributable to localized defects or imperfections but instead arises from the inherent structure and distribution of the fillers within the polymer matrix.

3.3. Tribological Results

Friction coefficient values for both CF and AC samples are illustrated in Figure 5a. The frictional response was recorded over 10,000 laps, during which a 6 mm alumina ball oscillated along a 4 mm stroke at a frequency of 2.5 Hz. While only a single curve is shown for each material, the data accurately reflect the general trend observed across all tested samples. As shown in Figure 5a, the recorded trends reveal distinct tribological behaviors that reflect the intrinsic material differences in structure, filler content, and surface response to sliding contact. During the initial running-in phase (0–1000 laps), both composites exhibited a steep increase in friction coefficient, characteristic of surface adaptation and contact area stabilization. CF samples began with a lower initial coefficient (~ 0.05 – 0.1) and a more gradual increase, while AC samples rapidly reached friction levels around ~ 0.5 within a few hundred cycles. This suggests a more compliant or smoother surface in CF, likely due to its more flexible matrix and lower filler content.

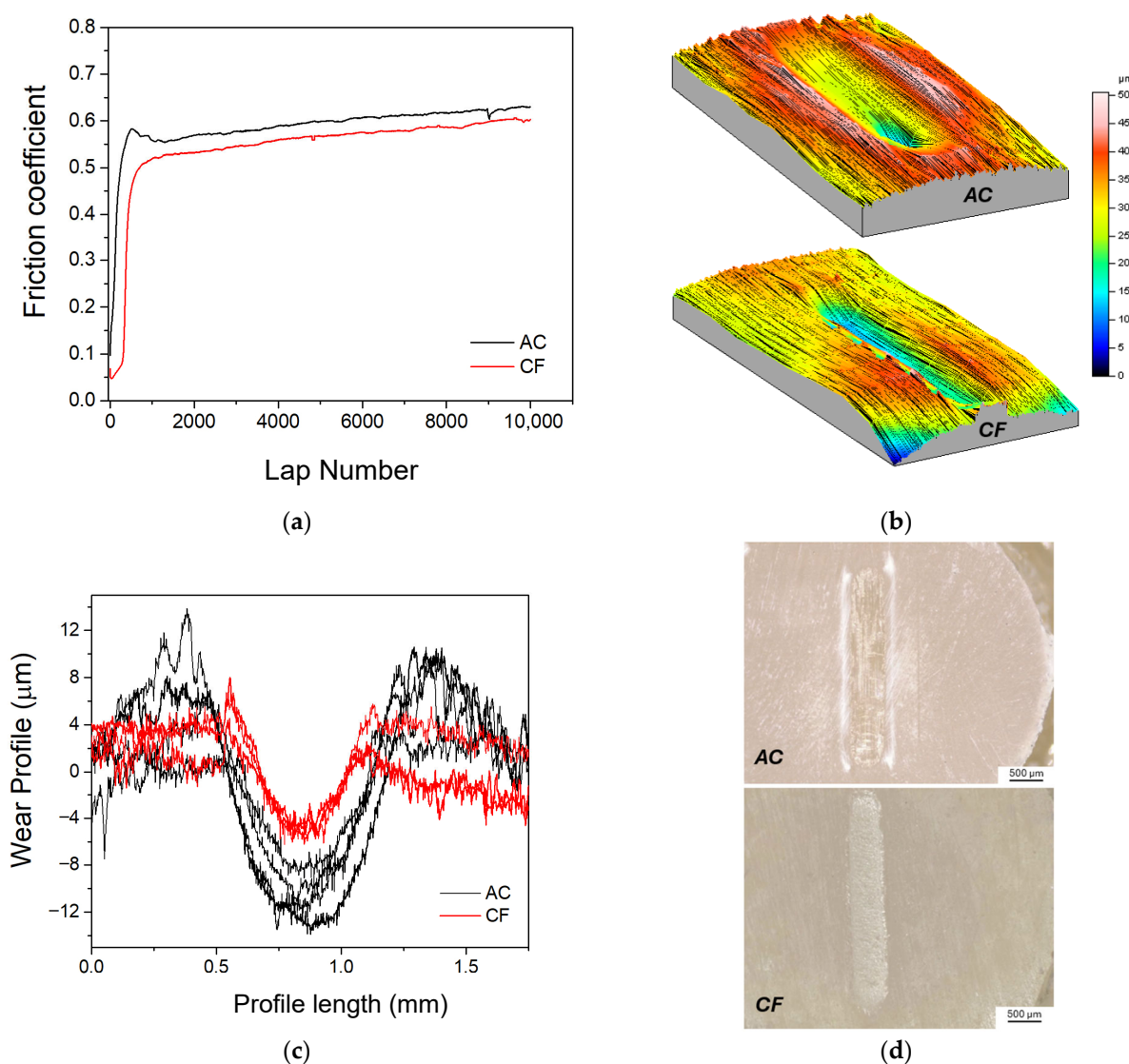


Figure 5. Representative curve of the friction coefficient for the composites (a), the 3D map reconstruction of the wear traces (b), the transverse profiles of the wear traces (c), and the macroscopic images by stereoscope of the wear traces (d).

However, a critical observation is that all CF samples prematurely interrupted the test. This interruption occurred because the friction force exceeded the upper safety threshold

set by the tribometer, indicating a sudden and significant rise in resistance to sliding. This abrupt frictional spike may be attributed to localized material accumulation, surface damage, or softening under repeated stress, which in turn could result in stick–slip behavior or partial adhesion to the counter-face (alumina ball). The described behavior underscores a lower thermal or mechanical stability of the CF composite under prolonged dynamic loading, despite its initially favorable frictional response.

In contrast, AC samples completed the full test duration of 10,000 cycles without exceeding operational limits. Although they exhibited a higher average friction coefficient (0.62 ± 0.060 compared to 0.55 ± 0.095 for CF), their behavior was more stable and progressive over time. The increase in friction was gradual and consistent, reflecting a more controlled wear mechanism. The AC composite, with its higher filler loading and greater crosslink density, resisted softening and maintained structural integrity throughout the test, albeit with slightly more pronounced surface wear.

Consequently, while CF demonstrated lower friction values initially, its tendency to reach critical frictional limits prematurely raises concerns about its reliability under long-term and high-load sliding conditions. On the other hand, AC's friction coefficient is higher but more stable in profile, along with its ability to endure the full testing cycle. This evidences its greater tribological robustness, making it potentially more suitable for clinical applications where durability and frictional endurance are critical.

The 3D reconstruction of the wear tracks after the tribological tests is shown in Figure 5b. The resulting surface maps revealed a slightly more pronounced deformation in AC, consistent with its higher frictional response. Nonetheless, the difference in surface degradation between the two materials was not significant.

Figure 5c displays the cross-sectional profiles of the worn regions, offering a direct comparison of wear depth. To further characterize surface damage, stereoscopic examination was conducted, providing high-resolution images of the wear tracks for both composites (Figure 5d). These observations, as well as the wear track reconstruction data reported in Table 3, confirmed the trends noted in the profilometric data and contributed to a comprehensive evaluation of wear performance. Although the worn surface areas were similar, the volumes involved and the maximum measured depths were found to be greater in AC compared to CF.

Table 3. Mean wear surface, volume, and max depth for the wear traces for both composites.

Sample	Wear Surface (mm ²)	Wear Volume (mm ³)	Max Depth (mm)
AC	1.82 ± 0.075	0.012 ± 0.0055	36.88 ± 3.642
CF	1.70 ± 0.159	0.0070 ± 0.0083	17.91 ± 3.387

Despite its higher strength, AC showed higher friction coefficients and greater wear volumes under reciprocating dry sliding (Table 3). This counterintuitive result indicates that higher filler content does not always equate to better wear resistance, especially in tribological systems where surface adaptability and energy dissipation play a crucial role. In particular, the higher presence of filler increases the abrasive component of wear, as evident in Figure 6, which reports the stereoscopic images of the abraded areas after the test and it clearly revealed evidence of abrasive wear. In the case of AC this wear is particularly pronounced, leading to regions of material loss caused by matrix deformation and tearing. As a result, filler particles released from the matrix contributed more actively to the wear process.

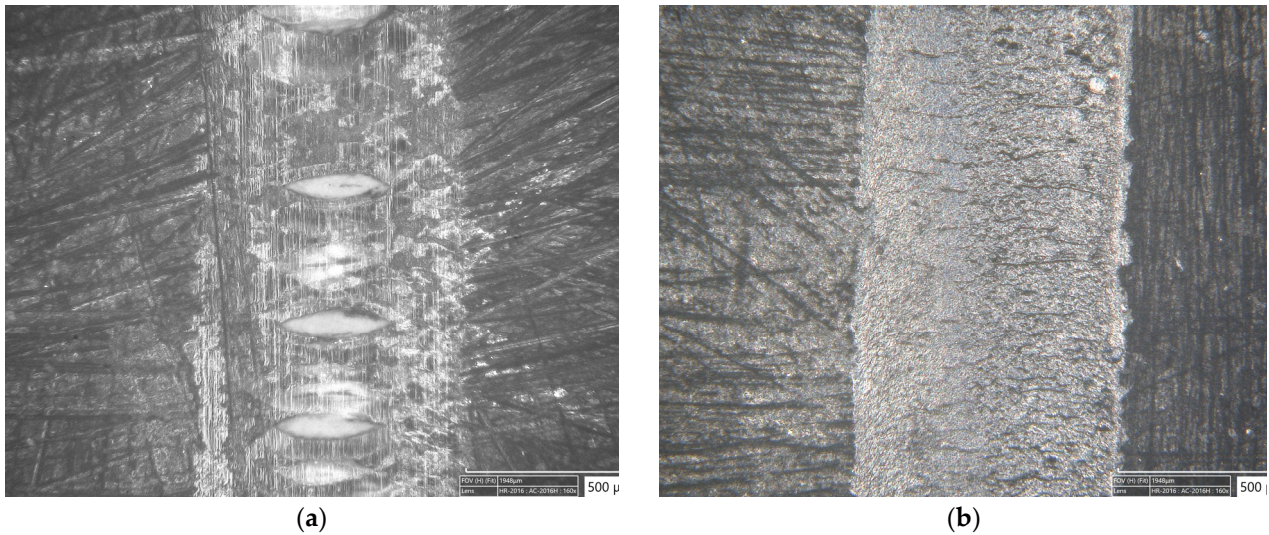


Figure 6. Magnifications on the stereoscope of the wear areas for the AC (a) and CF (b) composites.

CF demonstrated lower friction, reduced wear track depth, and overall better wear performance, despite its lower mechanical stiffness. One plausible explanation lies in its higher polymer content, which may act as a self-lubricating or energy-absorbing layer during sliding (Figure 6b). Furthermore, its more elastic matrix likely redistributes localized contact stresses more effectively, reducing crack initiation and propagation. This suggests that CF could be particularly effective for applications involving dynamic or shear-loaded interfaces, such as aligner–attachment contact points or interproximal guidance zones.

The results on wear behavior are further supported also by the surface roughness data before and after the wear test, as reported in Table 4. Before the test, the average surface roughness of the AC samples was higher than the CF samples. However, after the wear test the roughness in the worn area became comparable for the two materials. The results on wear behavior are further substantiated by the surface roughness measurements conducted before and after the wear test, as reported in Table 4. Prior to wear, the average surface roughness (Ra) and the total peak-to-valley height (Rt) of the AC samples were significantly higher than those of the CF samples, indicating a more irregular initial surface for the AC material. Specifically, the AC sample exhibited an Ra of $0.577 \pm 0.035 \mu\text{m}$ and an Rt of $4.369 \pm 0.521 \mu\text{m}$, compared to $0.337 \pm 0.070 \mu\text{m}$ and $2.862 \pm 0.549 \mu\text{m}$ for the CF sample.

Table 4. Roughness parameters (Ra and Rt) evaluated for AC and CF samples before and after wear tests.

Sample	Average Roughness (Ra, μm)		Total Peak to Valley Height (Rt, μm)	
	Unworn Zone	Worn Zone	Unworn Zone	Worn Zone
AC	0.577 ± 0.0352	0.247 ± 0.03649	4.369 ± 0.5206	2.537 ± 0.6496
CF	0.337 ± 0.0703	0.236 ± 0.0189	2.862 ± 0.5488	2.224 ± 0.7815

This initial difference is consistent with the observed abrasive wear behavior, which was more pronounced in the AC sample. After the wear test, both materials showed a notable decrease in surface roughness, with Ra values converging to $0.247 \pm 0.036 \mu\text{m}$ (AC) and $0.236 \pm 0.019 \mu\text{m}$ (CF), and Rt values reducing to $2.537 \pm 0.650 \mu\text{m}$ (AC) and $2.224 \pm 0.782 \mu\text{m}$ (CF). This convergence suggests that the wear process smoothed the surfaces, reducing the initial topographical differences.

4. Discussion

Attachment features represent one of the key components in clear aligner treatment (CAT), as they ensure proper aligner fit and precise control of planned movements [1,2,5]. Therefore, their accurate reproduction depends on the suitable selection of composite resins, which guarantee integrity and shape stability of these features throughout the treatment course [3,4,14]. Flowable and conventional resins are commonly used for attachment fabrication, despite differences in filler volume and viscosity. Although several authors [1,2,16] have reported superior performance of conventional resins, flowable materials reveal easier adaptation to the attachment template [16]. Recently, the introduction of hybrid composites—such as Aligner Connect (AC)—has enabled one to combine handling benefits of flowable materials with the mechanical strength of conventional composites, providing an alternative that may optimize both placement and long-term stability of attachments. Thus, this study aimed to evaluate and compare the mechanical, thermal, and tribological properties of two nanocomposite materials, Aligner Connect (AC) and Connect Flow (CF), characterized by different composition and viscosity. The investigation provided a thorough comparative analysis of these advanced light-cured nanocomposites using a tailored multi-scale testing protocol developed specifically for this type of application. The results emphasized the clinical relevance of composite selection to optimize the clinical performance of orthodontic attachments, as the materials' behavior under stress, wear, and temperature changes can significantly influence the predictability of tooth movement and aligner fit. Choosing an inappropriate composite may compromise the integrity of the attachment surface, leading to premature debonding, reduced aligner retention, or ineffective force transmission. This highlights the importance of characterizing not only the mechanical performance but also the thermal and tribological properties, which together determine the long-term clinical success of CAT. Overall, AC demonstrated better durability and structural reliability due to its greater mechanical strength, more stable stress relaxation, and increased filler content. All these characteristics represent key factors for achieving effective and long-lasting orthodontic outcomes. In particular, the higher filler content of AC (61%), as measured during the combustion test, appears to be one of the main contributors to its superior mechanical performance. Consistent with our findings, previous studies [16,17] have shown that low-viscosity composites with high filler loading exhibit enhanced mechanical properties. Increased filler content is generally associated with improved stiffness, enhanced load-bearing capacity, and improved wear resistance, also confirmed by the indentation test results. Thermal analysis further elucidated the structural differences between the materials [18]. Specifically, the AC composite, characterized by a higher inorganic filler content, exhibits greater thermal stability and a more rigid network architecture, as reflected in its broader glass transition and lower heat flow. In contrast, the CF composite demonstrates increased thermal activity, a sharper and lower T_g , and a more flexible polymer matrix, consistent with reduced filler loading. These differences highlight the critical role of filler content and matrix–filler interactions in influencing the thermal response, processability, and long-term stability of these composites. The ability of AC to maintain a stable structure under thermal fluctuations suggests a potential advantage in clinical conditions, where temperature changes from food and beverages may affect the integrity of attachments. CF, while less thermally stable, might benefit from a certain degree of flexibility which could reduce stress accumulation at the composite–tooth interface.

The hybrid nanocomposite AC consistently outperformed CF in terms of stiffness, load-bearing capacity, and structural integrity, showing nearly double the maximum indentation load and significantly higher elastic modulus values. Its high inorganic filler content contributed not only to increased mechanical robustness but also to greater dimensional stability under compressive loading. These properties make AC highly suitable for fabri-

cating precise and long-lasting orthodontic attachments, where mechanical demands are substantial and patient compliance must be optimized. As a matter of fact, instrumented flat indentation testing revealed that AC reached a maximum load of $586.47 \text{ N} \pm 25.02$ at a penetration depth of 0.3 mm, which was significantly higher than the $291.76 \text{ N} \pm 7.37$ recorded for CF. This indicates greater resistance to localized deformation, a critical property for preserving attachment integrity under forces generated by aligners and daily oral functions such as chewing [19]. With regard to tribological performance, CF exhibited superior behavior—including lower friction coefficients, reduced wear volume, and greater stress dissipation—highlighting its value in applications requiring flexibility, adaptive stress response, or sliding contact. Moreover, the more substantial reduction in both Ra and Rt for the AC sample supports the hypothesis of greater material removal by an abrasive phenomenon, which was also evident from the stereomicroscopic analysis. In contrast, the CF sample retained a more stable surface profile, consistent with its improved wear resistance. Overall, the roughness data corroborate the mechanical observations and provide quantitative insights into the differing wear mechanisms and material responses of the two samples. Despite its lower strength, CF's enhanced surface durability suggests that it may be preferable in areas prone to micromovement or repeated mechanical friction, such as aligner contact zones, interproximal spaces, or undercut regions. AC, on the other hand, exhibited a higher coefficient of friction (0.62 ± 0.060) compared to CF (0.55 ± 0.095), suggesting increased interfacial friction when in contact with aligner materials. However, wear testing showed no significant difference in surface wear between the two materials, indicating a comparable wear pattern despite AC's higher friction. This suggests that while AC may generate slightly more friction, it does not compromise wear resistance and may influence aligner seating over time. Supporting this interpretation, Roatkanjanaporn et al. [20] found no differences in wear volume between nanohybrid flowable and nanofilled sculptable composites after repeated aligner insertion/removal over 24 weeks and also reported no significant effects of composite type on mean retentive force. Similarly, Shaalan et al. [21] observed comparable clinical performance between flowable and conventional composites after a 3 year follow-up. These findings reinforce the importance of integrating thermal, mechanical, and tribological evaluations in the selection of orthodontic composite materials, ensuring optimal treatment effectiveness and durability over time.

4.1. Clinical Perspective

From a clinical perspective, material choice should be aligned with the specific functional and biomechanical demands of each case. For scenarios requiring high retention, complex movements, and reduced deformation risk, AC appears to be the most suitable option. Conversely, CF may still be advantageous for less mechanically demanding treatments or where ease of handling, improved adaptation to templates, and reduced interfacial friction are prioritized, such as for attachments in interproximal or undercut regions. Clinicians should also consider patient-specific factors, including aligner replacement intervals, dietary habits, and oral hygiene routines, which may impact the longevity and wear behavior of the chosen composite.

4.2. Strength, Limitations and Future Directions

This study introduces a novel experimental protocol for the systematic characterization of dental composites at clinically relevant dimensions, incorporating custom photomasks, layer-specific curing, and multi-modal mechanical testing. However, the in vitro design of the experimental analysis does not fully replicate the complex oral environment, including variations in humidity, pH, enzymatic activity, and temperature. Furthermore, cyclic loading, aging effects such as thermocycling, and long-term fatigue behavior were not

simulated, which may affect the real-world durability of these composites. Future work may extend these findings by evaluating the composites' performance under simulated oral conditions, such as thermocycling, moisture exposure, and fatigue loading. Additionally, *in vivo* studies will be essential to confirm how these laboratory-measured differences translate into real-world clinical outcomes over the course of orthodontic treatment.

5. Conclusions

The mechanical, thermal, and tribological characterization performed in this study highlights the decisive influence of material composition on the performance of orthodontic attachments. The hybrid nanocomposite Aligner Connect (AC) demonstrated significantly superior performance compared to the flowable resin Connect Flow (CF), showing nearly double the maximum indentation load and a notably higher elastic modulus. The increased inorganic filler content of AC not only enhanced its mechanical strength but also improved its dimensional stability under compressive loading. These findings underscore that the most clinically relevant result of this study is the superior load-bearing capacity and long-term structural integrity of AC, which makes it a particularly suitable choice for cases requiring high retention and precise tooth movements.

Moreover, the tribological analysis revealed that CF, while less rigid, exhibited lower friction coefficients and improved surface wear resistance, suggesting that its use may be preferable in less mechanically demanding clinical situations or where better adaptability to the aligner template is needed. This study therefore provides clinically meaningful guidance for selecting composite materials tailored to the biomechanical requirements of clear aligner treatments.

The proposed experimental protocol, which integrates custom photomasks, layer-specific curing, and multi-modal mechanical testing, represents a novel and reproducible methodology for the evaluation of next-generation orthodontic materials. However, the *in vitro* conditions of experimental analysis do not fully replicate the complex oral environment, including thermal cycling, humidity, and masticatory loads, which may influence long-term material performance. Moreover, only two materials were tested, which limits the generalizability of the conclusions.

Future research should focus on validating these findings under clinically simulated conditions, such as extended fatigue testing and thermocycling, and on conducting *in vivo* studies to assess the long-term behavior of attachment materials during actual orthodontic treatments. Such investigations will help to translate the present laboratory findings into concrete clinical recommendations and further improve the predictability and success of clear aligner therapies.

Author Contributions: Conceptualization, F.G. and R.L.; methodology, D.B.; validation, D.B., L.S. and P.C.; investigation, C.P.; writing—original draft preparation, F.G. and D.B.; writing—review and editing, R.L.; supervision, P.C. and L.S. All authors have read and agreed to the published version of the manuscript.

Funding: This research received no external funding.

Institutional Review Board Statement: Not applicable.

Informed Consent Statement: Not applicable.

Data Availability Statement: The original contributions presented in this study are included in the article. Further inquiries can be directed to the corresponding author.

Conflicts of Interest: The authors declare no conflicts of interest.

Abbreviations

The following abbreviations are used in this manuscript:

CAT	Clear Aligner Treatment
AC	Aligner Connect
CF	Connect Flow
DSC	Differential Scanning Calorimetry
3D	Three-Dimensional
Tg	Glass Transition Temperature
C	Celsius
N	Newton
MPa	MegaPascal
mm	Millimeter
µm	Micrometer
Ra	Average Roughness
Rt	Total peak to valley height
PLA	Polyactic Acid
LED	Light-Emitting Diode
mW	milliWatt
cm	Centimeter
mg	Milligram
min	Minutes
kN	kiloNewton

References

- Gazzani, F.; Bellisario, D.; Quadrini, F.; Danesi, C.; Alberti, A.; Cozza, P.; Pavoni, C. Light-curing process for clear aligners' attachment reproduction: Comparison between two nanocomposites cured by the auxiliary of a new tool. *BMC Oral Health* **2022**, *22*, 376. [[CrossRef](#)] [[PubMed](#)]
- Gazzani, F.; Bellisario, D.; Quadrini, F.; Parrinello, F.; Pavoni, C.; Cozza, P.; Lione, R. Comparison between different composite resins used for clear aligner attachments: An in-vitro. *Front. Mater.* **2022**, *8*, 789143. [[CrossRef](#)]
- Morton, J.; Derakhshan, M.; Kaza, S.; Li, C. Design of the Invisalign System Performance. *Semin. Orthod.* **2017**, *23*, 3–11. [[CrossRef](#)]
- D'Antò, V.; Muraglie, S.; Castellano, B.; Candida, E.; Sfondrini, M.F.; Scribante, A.; Grippaudo, C. Influence of Dental Composite Viscosity in Attachment. Reproduction: An Experimental In Vitro Study. *Materials* **2019**, *12*, 4001. [[CrossRef](#)] [[PubMed](#)]
- Mantovani, E.; Castroflorio, E.; Rossini, G.; Garino, F.; Cugliari, G.; Deregibus, A.; Castroflorio, T. Scanning electron microscopy analysis of aligner fitting on anchorage attachments. *J. Orofac. Orthop.* **2019**, *80*, 79–87. [[CrossRef](#)] [[PubMed](#)]
- Weckmann, J.; Scharf, S.; Graf, I.; Schwarze j Keilig, L.; Bourauel, C.; Braumann, B. Influence of attachment bonding protocol on precision of the attachment in aligner treatments. *J. Orofac. Orthop.* **2020**, *81*, 30–40. [[CrossRef](#)] [[PubMed](#)]
- Kravitz, N.D.; Kusnoto, B.; Agran, B.; Viana, G. Influence of attachments and interproximal reduction on the accuracy of canine rotation with invisalign. A prospective clinical study. *Angle Orthod.* **2008**, *78*, 682–687. [[CrossRef](#)] [[PubMed](#)]
- Dasy, H.; Dasy, A.; Asatrian, G.; Rózsa, N.; Lee, H.F.; Kwak, J.H. Effects of variable attachment shapes and aligner material on aligner retention. *Angle Orthod.* **2015**, *85*, 934–940. [[CrossRef](#)] [[PubMed](#)]
- Kusai Baroudi, J.C.R. Flowable resin composites: A systematic review and clinical considerations. *J. Clin. Diagn. Res.* **2015**, *9*, ZE18–ZE24. [[CrossRef](#)] [[PubMed](#)]
- Barreda, G.J.; Dzierewianko, E.A.; Munoz, K.A.; Piccoli, G.I. Surface wear of resin composites used for Invisalign® attachments. *Acta Odontol. Latinoam.* **2017**, *30*, 90–95. [[PubMed](#)]
- Bowman Feinberg, K.; Souccar, N.M.; Kau, C.H.; Oster, R.A.; Lawson, N.C. Translucency, Stain Resistance, and Hardness of composites used for Invisalign Attachments. *JCO* **2016**, *3*, 170–176.
- Aminoroaya, A.; Neisiany, R.E.; Khorasani, S.N.; Panahi, P.; Das, O.; Madry, H.; Cucchiari, M.; Ramakrishna, S. A review of dental composites: Challenges, chemistry aspects, filler influences, and future insights. *Compos. B Eng.* **2021**, *216*, 108852. [[CrossRef](#)]
- Ferracane, J.L. Resin Composite-State of the Art. *Dent. Mater.* **2011**, *27*, 29–38. [[CrossRef](#)] [[PubMed](#)]
- Bruno, G.; Gracco, A.; Barone, M.; Mutinelli, S.; De Stefani, A. Invisalign® vs. Spark™ template: Which is the most effective in the attachment bonding procedure? A randomized controlled trial. *Appl. Sci.* **2021**, *11*, 6716. [[CrossRef](#)]

15. Simon, M.; Keilig, L.; Schwarze, J.; Jung, B.A.; Bourauel, C. Treatment outcome and efficacy of an aligner technique—Regarding incisor torque, premolar derotation and molar distalization. *BMC Oral Health* **2014**, *14*, 68. [[CrossRef](#)] [[PubMed](#)]
16. Clelland, N.L.; Pagnotto, M.P.; Kerby, R.E.; Seghi, R.R. Relative wear of flowable and highly filled composite. *J. Prosthet. Dent.* **2004**, *93*, 153–157. [[CrossRef](#)] [[PubMed](#)]
17. Ocak, I.; Gorucu-Coskuner, H.; Aksu, M. Wear resistance of orthodontic attachments: A comparative analysis of different composite resins in clear aligner therapy. *Clin. Oral Investig.* **2025**, *29*, 242. [[CrossRef](#)] [[PubMed](#)]
18. Bansal, G.; Gautam, R.K.; Misra, J.P.; Kishore, C.; Mishra, A.; Verma, A. Evaluation of mechanical and thermal properties of thermosetting polymer composites. In *Dynamic Mechanical and Creep-Recovery Behavior of Polymer-Based Composites*; Elsevier: Amsterdam, The Netherlands, 2024; pp. 53–68.
19. Li, Q.; Yang, K. Surface wear of attachments in patients during clear aligner therapy: A prospective clinical study. *Prog. Orthod.* **2024**, *25*, 7. [[CrossRef](#)] [[PubMed](#)]
20. Roatkanjanaporn, N.; Chavanavesh, J.; Teekavanich, C. Wear volumes of flowable and sculptable resin composite attachments and their correlation with retentive force of clear aligners: A laboratory study. *BMC Oral Health* **2025**, *25*, 483. [[CrossRef](#)] [[PubMed](#)]
21. Shaalan, O.O.; Abou-Auf, E.; El Zoghby, A.F. Clinical evaluation of flowable resin composite versus conventional resin composite in carious and noncarious lesions: Systematic review and meta-analysis. *J. Conserv. Dent.* **2017**, *20*, 380–385. [[CrossRef](#)] [[PubMed](#)]

Disclaimer/Publisher’s Note: The statements, opinions and data contained in all publications are solely those of the individual author(s) and contributor(s) and not of MDPI and/or the editor(s). MDPI and/or the editor(s) disclaim responsibility for any injury to people or property resulting from any ideas, methods, instructions or products referred to in the content.